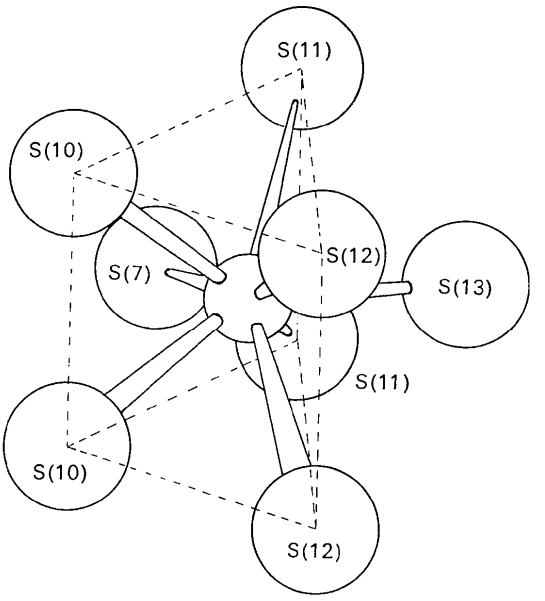

Fig. 4. Environment de l'atome de La(8).

cette dernière, les atomes d'yttrium de coordinence 6 ont des environnements identiques aux atomes d'erbium et les atomes d'yttrium de coordinence 7 sont dans les mêmes sites que les atomes de lanthane.

Il est intéressant de se demander pourquoi l'affinement n'a pas voulu converger au départ dans le groupe $B2/m$. Nous avons alors comparé les coordonnées des atomes lourds adoptées au début de l'étude de cette structure avec celles trouvées à la fin de l'affinement. Les écarts sont assez importants, allant jusqu'à 0,02 sur x et sur y. Dans ces conditions l'affinement dans le groupe centrosymétrique $B2/m$ ne converge pas.

Nous avons déjà, dans d'autres cas, constaté empiriquement que le programme d'affinement, qui est une adaptation du programme de Busing, Martin & Levy (1962) et qui utilise la matrice complète des équations normales dans la méthode des moindres carrés ne convergeait pas quand les données étaient un peu trop éloignées de la bonne valeur. Mais il n'était pas arrivé que des données exactes à 0·02 près ne conduisent pas à la solution. Cela tient sans doute, dans notre cas, au nombre élevé d'atomes lourds dans l'unité asymétrique (10) qui obligeait à prendre d'emblée 18 paramètres variables.

Conclusion

Le caractère dominant de cette structure est certainement la grande différenciation qui s'opère entre les atomes de lanthane et les atomes d'erbium, aussi bien du point de vue de l'environnement que des distances interatomiques. La comparaison de cette maille avec celle de Y_5S_7 (Adolphe, 1965) met en évidence une certaine ressemblance entre ces deux structures; dans

References

ADOLPHE, C. (1965). *Ann. Chim.* **10**, 271–275.
BUSING, W. R., MARTIN, K. O. & LEVY, H. A. (1962). *ORFLS*. Report ORNL-TM-305. Oak Ridge National Laboratory, Oak Ridge, Tennessee.
CROMER, D. T. & WABER, J. T. (1965). *Acta Cryst.* **18**, 104–109.
KHODADAD, P. & VO VAN TIEN (1969). *Soc. Chim. Fr.* pp. 30–39.

Acta Cryst. (1973). B**29**, 73

The Crystal Structure of Scawtite, $Ca_7(Si_6O_{18})(CO_3).2H_2O$

BY J. J. PLUTH AND J.V. SMITH

Department of the Geophysical Sciences, The University of Chicago, Chicago, Illinois, 60637, *U.S.A.*

(*Received* 20 *April* 1972; *accepted* 15 *September* 1972)

Scawtite contains 2 units of $Ca_7(Si_6O_{18})(CO_3).2H_2O$ in a monoclinic cell with $a=10{\cdot}118$ (3), $b=15{\cdot}187$ (4), $c=6{\cdot}626$ (1) Å and $\beta=100°40$ (1)′. Structure refinement in space group $I2/m$ was satisfactory for most of the structure, but problems with the CO_3 groups require either disorder or an ordered pattern in a lower space group, perhaps Im. The scawtite structure consists of layers of octahedrally coordinated calcium atoms alternating with layers of Si_6O_{18} rings and CO_3 triangles. The water molecules belong to calcium octahedra.

Introduction

Scawtite is the third member of the calcium carbonate silicate group of minerals. The crystal structure of tilleyite, $Ca_5(Si_2O_7)(CO_3)_2$, was determined by Smith (1953) and refined by Louisnathan & Smith (1970). It consists of corrugated walls of linked calcium–oxygen octahedra and Si_2O_7 groups cross-linked by calcium–oxygen octahedra and CO_3 triangles. The crystal structure of spurrite, $Ca_5(SiO_4)_2CO_3$, was deter-

mined and described by Smith, Karle, Hauptman & Karle (1960). It consists of a pseudo-hexagonal pattern of SiO_4 tetrahedra and CO_3 triangles linked by Ca atoms in irregular polyhedra. Chao (1972) described the crystal structure of carletonite,

$$KNa_4Ca_4Si_8O_{18}(CO_3)_4(F,OH).H_2O,$$

a new mineral from Mount St. Hilaire, Quebec. Carletonite has a layered structure containing two carbonate layers and an Si_8O_{18} double sheet.

McConnell (1955) determined the properties of scawtite from Ballycraigy, Larne, N. Ireland as $a=6{\cdot}61$, $b=15{\cdot}22$, $c=10{\cdot}98$ Å, $\beta=115°24'$, $n_\alpha=1{\cdot}595$, $n_\beta=1{\cdot}605$, $n_\gamma=1{\cdot}622$, $2V+75°$; $Y=b$, $Z\wedge\mathbf{a}=30°$ and $Z\wedge\mathbf{c}$ 34°; $2[Ca_6Si_6O_{18}2H_2O.CaCO_3]$ for an A-centered cell. Murdoch (1955) found consistent data for scawtite from Crestmore, California: $a=10{\cdot}22$, $b=15{\cdot}42$, $c=6{\cdot}70$ Å, $\beta=100°29'$, probable space group $I2/m$; dominant forms {100}, {110}, {120}, {130}, {010} and {101}. From powder photographs, McConnell found that scawtite broke down to wollastonite upon heating to 850 °C. The transformation matrix from the A cell to the I cell is $-101/010/100$ with $Y=b$, $Z\wedge\mathbf{a}=70°$ and $Z\wedge\mathbf{c}=30°$.

Experimental

A sample of scawtite from Ballycraigy, Larne, N. Ireland, kindly provided by Dr S. O. Agrell of Cambridge University, proved too fine-grained for single-crystal X-ray study. A sample from Crestmore, California provided by Dr Paul B. Moore of the University of Chicago, yielded suitable crystals. A spectral scan on an electron microprobe showed no elements other than Ca and Si for wavelengths under 10 Å, and the chemical formula given by McConnell was assumed to be correct.

Weissenberg and precession photographs confirmed the cell dimensions and space groups given by Murdoch and McConnell. The cell chosen has an I lattice.

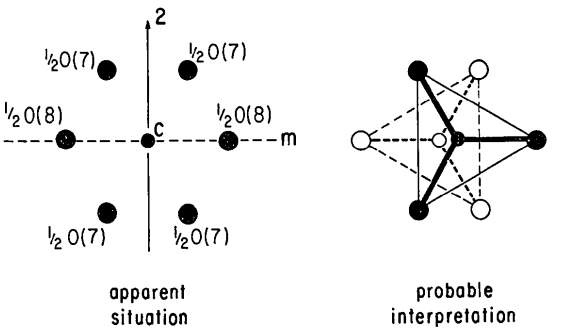

Fig. 1. Schematic drawing showing the apparent situation around the C atom, and a probable interpretation in terms of two positions for the CO_3 group.

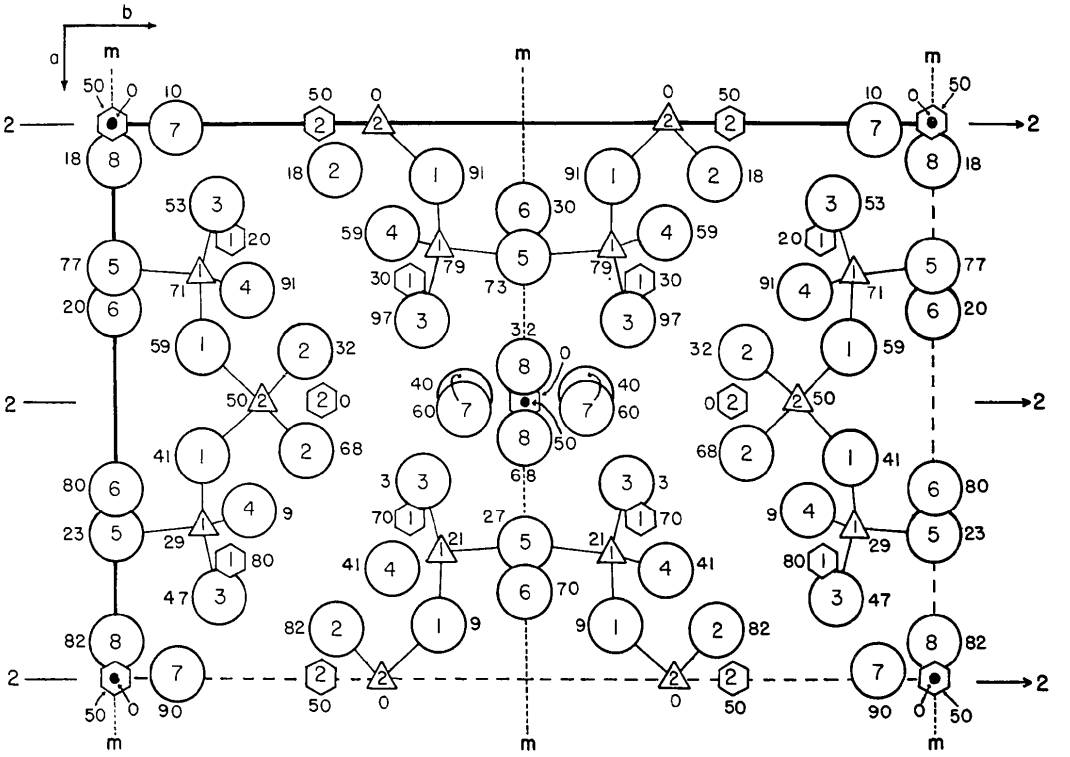

Fig. 2. Projection onto (001) showing the unit-cell contents. The oxygen, silicon, calcium and carbon atoms are represented by large circles, triangles, hexagons and small dots respectively. Positions in percentage of the **c** repeat are indicated near atom symbols.

Table 1. *Observed and calculated structure factors*

Unit-cell parameters and their estimated errors were obtained by least-squares adjustment of twenty-five $1/d^2$ values using a program written by Burnham (1962). These d spacings, measured from a Guinier photograph taken at room temperature using quartz-monochromatized Fe $K\alpha$ radiation ($\lambda = 1{\cdot}9373$ Å) and a spinel standard ($a = 8{\cdot}0800$) gave $a = 10{\cdot}118$ (3), $b = 15{\cdot}187$ (4), $c = 6{\cdot}626$ (1), and $\beta = 100°40$ (1)′.

A transparent rectangular parallelepiped with dimensions $0{\cdot}10 \times 0{\cdot}13 \times 0{\cdot}15$ mm was mounted on a Picker-FACS-1 four-circle diffractometer with its b axis slightly offset from the φ axis and 1875 symmetry-independent reflections $\{[(\sin\theta)/\lambda]_{max} = 0{\cdot}756\}$ were measured with θ–2θ scans using graphite-monochromatized Mo $K\alpha$ radiation ($\lambda = 0{\cdot}71069$ Å).

The intensity data were corrected for Lorentz and polarization effects, but no absorption correction was applied because the crystal was small and equidimensional and the linear absorption parameter was 22·3 cm^{-1}.

The estimated errors in the intensities (σ_I) were calculated using

$$\sigma_I = [S + t^2B + k^2(S + tB)^2]^{1/2},$$

with S = peak scan counts, B = total background counts, t = ratio of peak to background observation times, and k = instability constant = 0·008 which was estimated from repeated measurements of standard reflections. These σ_I's were converted to the estimated errors in the relative structure factors (σ_F) by

$$\sigma_F = [(I + \sigma_I)/\mathrm{Lp}]^{1/2} - (I/\mathrm{Lp})^{1/2}$$

with I = relative intensity and Lp = Lorentz and polarization factors.

Structure determination and refinement

Initial phases were assigned from a structure-factor calculation using three calcium positions derived from a Patterson synthesis. A zero-moment test to decide between the space groups Im, $I2$ and $I2/m$ proved inconclusive, and the trial model was refined using the space group $I2/m$. After Fourier and least-squares refinement (*ORFLS*) all atoms except hydrogen were located and the final cycle of least-squares refinement minimized $\sum w||F_o| - |F_c||^2$ with $w = (1/\sigma_F)^2$. Using isotropic B values, the maximum parameter shift was $0{\cdot}2\sigma$ while $R = 0{\cdot}117$, $R_w = 0{\cdot}103$ and $S = 7{\cdot}87$ where

$$\begin{aligned} R &= \textstyle\sum||F_o| - |F_c||/\sum|F_o| \\ R_w &= [\textstyle\sum w||F_o| - |F_c||^2/\sum w|F_o|^2]^{1/2} \\ S &= [(\textstyle\sum w||F_o| - |F_c||^2)/(n_o - n_v)]^{1/2} \\ n_o &= \text{number of reflections} \\ n_v &= \text{number of parameters.} \end{aligned}$$

At this point a difference Fourier synthesis was calculated which contained significant peaks (4·6 and 1·6 e $Å^{-3}$) near Ca(3) and Ca(1), both of which are bonded to oxygen atoms of the CO_3, and near O(7), part of the CO_3 group itself. Anisotropic thermal parameters were introduced into the least-squares refinement with the final cycle having a maximum param-

Table 2. *Positional and thermal parameters in I2/m*

Standard error in brackets applies to same significance level as last figure.

	x/a	y/b	z/c	B†
Ca(1)	0·2120 (1)	0·1402 (1)	0·1996 (2)	1·00 (2)
Ca(2)	½	0·2495 (1)	0	0·66 (3)
Ca(3)	½	½	0	1·39 (5)
Si(1)	0·7729 (1)	0·3957 (1)	0·2059 (2)	0·45 (3)
Si(2)	0	0·3233 (1)	0	0·46 (4)
O(1)	0·9028 (4)	0·3933 (3)	0·0901 (6)	1·13 (8)
O(2)	0·0879 (4)	0·2683 (3)	0·1837 (6)	0·89 (8)
O(3)	0·6447 (4)	0·3756 (3)	0·0322 (6)	0·84 (7)
O(4)	0·6980 (4)	0·1619 (2)	0·0918 (6)	0·74 (7)
O(5)	0·7409 (6)	0	0·2268 (8)	0·83 (10)
O(6) [H_2O]	0·3452 (7)	0	0·2033 (9)	1·66 (13)
C	0	0	0	1·46 (24)
O(7)*	0·0152 (12)	0·0699 (9)	0·1024 (20)	4·04 (33)
O(8)*	0·0665 (13)	0	0·1777 (18)	1·47 (25)

* O(7) and O(8) were assigned an occupancy of 0·5.
† B's are from an isotropic thermal parameter refinement.

Table 3. *Anisotropic thermal parameters*

The thermal parameters are defined as $\exp[-\frac{1}{4}\sum_{j=1}^{3}\sum_{i=1}^{3} B_{ij}h_ih_ja_i^*a_j^*]$.

	B_{11}	B_{22}	B_{33}	B_{12}	B_{13}	B_{23}
Ca(1)	1·26 (4)	0·91 (4)	1·09 (4)	0·29 (3)	0·54 (3)	0·33 (3)
Ca(2)	0·71 (5)	0·42 (5)	0·88 (5)	0	0·25 (4)	0
Ca(3)	1·41 (9)	0·27 (7)	3·24 (12)	0	1·39 (9)	0
Si(1)	0·57 (5)	0·42 (5)	0·41 (5)	0·08 (4)	0·03 (3)	−0·04 (4)
Si(2)	0·53 (7)	0·51 (7)	0·44 (7)	0	0·03 (5)	0
O(1)	0·96 (14)	1·06 (15)	1·55 (16)	0·36 (12)	0·62 (12)	0·24 (13)
O(2)	1·06 (14)	1·02 (15)	0·61 (13)	0·34 (12)	−0·04 (11)	0·00 (11)
O(3)	0·74 (13)	0·74 (13)	1·04 (14)	0·02 (11)	−0·16 (11)	−0·13 (12)
O(4)	1·09 (14)	0·36 (13)	0·84 (14)	0·33 (11)	0·15 (11)	0·23 (11)
O(5)	1·37 (22)	0·35 (18)	1·04 (21)	0	0·69 (17)	0
O(6)	2·77 (30)	1·09 (23)	1·08 (23)	0	−0·02 (21)	0
C	0·54 (38)	3·07 (60)	1·09 (44)	0	−0·07 (32)	0
O(7)†	3·15 (55)	6·84 (75)	6·20 (74)	−3·72 (59)	2·53 (59)	−5·78 (63)
O(8)	1·25 (49)	2·58 (61)	0·66 (43)	0	0·03 (36)	0

† Not positive definite.

eter shift of $1{\cdot}2\sigma$ and $R=0{\cdot}083$, $R_w=0{\cdot}074$ and $S=6{\cdot}2$. A final difference Fourier synthesis contained no significant residual peaks. Atomic scattering factors for Ca^{2+}, Si^{2+}, O^- and C (Cromer & Mann, 1968) were used with anomalous scattering corrections for Ca^{2+} and Si^{2+} (Cromer, 1965).

The crystal structure shows one severe problem (Fig. 1). The C atom lies at the intersection of a mirror plane and a twofold axis, and has six oxygen neighbors, two O(8) atoms and four O(7) atoms all of half-weight (left-hand diagram). Such a distribution is incompatible with the expected occurrence of C in an equilateral triangle of oxygens. However the model in the right-hand diagram of Fig. 1 is plausible. The C atom actually bonds to two O(7) atoms and one O(8) atom to form the expected triangle, in either or both of two orientations. Either scawtite is fully ordered with possible space group *Im*, or it is disordered in *I*2/*m*. For the latter, there are two orientations of the CO_3 group as shown by continuous and dashed lines, while for the former, the apparent distribution is merely a mathematical consequence of assuming *I*2/*m* symmetry.

One complete cycle of least-squares refinement was made for *Im* in which atoms related by the twofold axis were separated into two blocks, and each block was varied while the other block was held constant. Because R increased from 0·138 to 0·150, refinement in *Im* was abandoned.

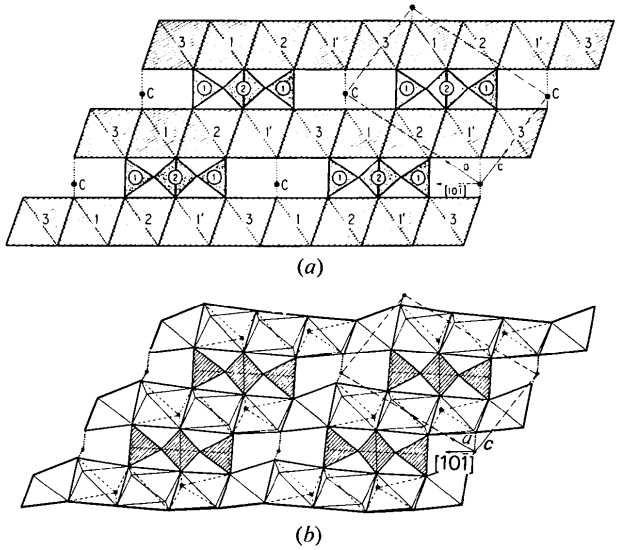

(*a*)

(*b*)

Fig. 3. Idealized (*a*) and actual (*b*) projections down the *b* axis. In the idealized projection, layers of polyhedra may be seen lying in (101). The hatched layer represents calcium–oxygen polyhedra severely idealized to regular octahedra sharing edges. Six silicate tetrahedra (shared) are linked to form Si_6O_{18} rings, which overlap in projection to show only three. The dotted line shows an end-on view of the CO_3 triangles and the solid squares in (*b*) represent water molecules. One unit cell is outlined by the dashed lines. In the actual projection, it may be seen that the calcium–oxygen polyhedra are very distorted. Note that for the type-2 octahedron, two vertices point in the same direction whereas for type 1, the two vertices point in opposite directions.

Table 4. *Interatomic distances and angles*

Si_6O_{18} rings

Si–O distances			
Si(1)–O*(1)	1·641 (4) Å	2Si(2)–O*(1)	1·635 (4) Å
Si(1)–O(3)	1·596 (4)	2Si(2)–O(2)	1·603 (4)
Si(1)–O(4)	1·582 (4)		
Si(1)–O*(5)	1·658 (2)		
O–O distances			
Si(1) tetrahedron		Si(2) tetrahedron	
O(1)–O(3)	2·582 (5) Å	O(1)–O(1′)	2·482 (8) Å
O(1)–O(4)	2·642 (5)	O(1)–O(2)	2·659 (5)
O(1)–O(5)	2·620 (6)	O(1)–O(2′)	2·640 (6)
O(3)–O(4)	2·756 (5)	O(2)–O(2′)	2·737 (7)
O(3)–O(5)	2·603 (5)		
O(4)–O(5)	2·625 (4)		
O–Si–O angles		**Si–O–Si angles**	
O(1)–Si(1)–O(3)	105·8 (2)°	Si(1)–O(5)–Si(1′)	145·5 (4)°
O(1)–Si(1)–O(4)	110·1 (2)	Si(1)–O(1)–Si(2)	140·7 (3)
O(1)–Si(1)–O(5)	105·2 (2)		
O(3)–Si(1)–O(4)	120·2 (2)		
O(3)–Si(1)–O(5)	106·2 (3)		
O(4)–Si(1)–O(5)	108·2 (2)		
O(1)–Si(2)–O(1′)	98·8 (3)		
O(1)–Si(2)–O(2)	110·4 (2)		
O(1)–Si(2)–O(2′)	109·2 (2)		
O(2)–Si(2)–O(2′)	117·2 (3)		
Ca–O distances			
Ca(1)–O(2)	2·307 (4) Å	2Ca(2)–O(2)	2·438 (4) Å
Ca(1)–O(2′)	2·459 (4)	2Ca(2)–O(3)	2·396 (4)
Ca(1)–O(3)	2·436 (4)	2Ca(2)–O(4)	2·388 (4)
Ca(1)–O(4)	2·306 (4)	4Ca(3)–O(3)	2·376 (4)
Ca(1)–O(6)	2·517 (4)	2Ca(3)–O(5)	2·898 (6)
Ca(1)–O(7)	2·247 (11)	4,2,0Ca(3)–O(7)	2·871 (14)
Ca(1)–O(8)	2·578 (7)	0,1,2Ca(3)–O(8)	2·355 (12)
Ca(1)–O(7′)	2·954 (15)		
O–O distances of coordination polyhedra			
Ca(1)			
O(2)–O(2′)†	3·282 (8) Å	O(3)–O(6)	3·751 (7) Å
O(2)–O(3)†	3·154 (5)	O(3)–O(7)†	3·023 (12)
O(2)–O(4)	3·478 (5)	O(3)–O(8)†	3·004 (10)
O(2)–O(7)	3·126 (13)	O(4)–O(6)	3·122 (5)
O(2)–O(8)	4·080 (4)	O(4)–O(7)	3·663 (12)
O(2′)–O(3)	3·668 (6)	O(4)–O(8)	4·060 (10)
O(2′)–O(4)†	2·926 (5)	O(6)–O(7)	3·449 (15)
O(2′)–O(6)	3·635 (4)	O(6)–O(8)†	2·793 (15)
Ca(2)			
O(2)–O(3)	3·937 (6) Å	O(3)–O(3′)†	2·880 (7) Å
O(2)–O(3′)†	3·154 (5)	O(3)–O(4)	3·302 (5)
O(2)–O(4)	3·647 (5)	O(4)–O(4′)	3·967 (7)
O(2)–O(4′)†	2·926 (5)		
Ca(3)			
O(3)–O(3′)†	2·880 (7) Å	O(3′)–O(7)†	3·023 (12) Å
O(3)–O(3″)	3·779 (8)	O(3′)–O(7′)	4·142 (17)
O(3)–O(5)	2·603 (5)	O(3′)–O(8)	3·654 (11)
O(3)–O(5′)	4·616 (7)	O(5)–O(7)	4·788 (16)
O(3)–O(7)	3·258 (12)	O(5)–O(8)	3·370 (14)
O(3)–O(7′)	4·317 (15)	O(5′)–O(7)	3·218 (12)
O(3)–O(8)†	3·004 (10)	O(5′)–O(8)	3·593 (13)

CO_3 group

C–O distances		O–O distances	
2C–O(7)	1·253 (11) Å	O(7)–O(7′)	2·122 (28) Å
C–O(8)	1·243 (12)	O(7)–O(8)	2·164 (14)
O–C–O angles			
O(7)–C–O(8)	120·2 (7)°		
O(7)–C–O(7′)	115·7 (14)		

* Bridging oxygen atoms.
† Shared edges.

The thermal parameters of the O(7), O(8) and C atoms in the *I*2/*m* refinement are larger than expected but only small movements near 0·1 to 0·2 Å from the mean position are required to give the higher *B* values. Neither diffuseness of Bragg diffractions nor presence of subsidiary diffractions were observed in Weissenberg and precession photographs. Consequently either random disorder in *I*2/*m* or complete order in *Im* are possible. All the data in the tables are given for random disorder in *I*2/*m* whereas the figures are drawn for an ordered arrangement in *Im*. Fig. 2 is a projection on (001).

The results of the anisotropic refinement in *I*2/*m* are given in Table 1 (structure factors), Tables 2 and 3 (atomic and thermal parameters) and Table 4 (bond distances and angles with errors from *ORFFE*).

Discussion

The scawtite structure consists essentially of alternating layers of octahedrally coordinated calcium atoms and of Si_6O_{18} rings lying parallel to (101). The water molecules are bonded to Ca atoms forming part of the calcium–oxygen layer. The CO_3 groups occupy space between the Si_6O_{18} rings.

Fig. 3 shows a projection onto (010) where diagram (*a*) is an idealized projection and (*b*) shows the actual atomic positions. Each Si_6O_{18} ring is bisected by the mirror plane of *I*2/*m*, and each stippled tetrahedron is the superposition of two tetrahedra. Two Si(1) tetrahedra link across the mirror plane and are joined by Si(2) tetrahedra to another pair of Si(1) tetrahedra.

The linkage of the oxygen octahedra about calcium is very complex in spite of the deceptive simplicity of the octahedral layer in Fig. 3, diagram (*a*). This idealized drawing gives the impression of a close-packed layer of regular octahedra sharing edges. Actually [diagram (*b*)] the calcium–oxygen polyhedra are very irregular, the layer is not continuous, and the topologic relation is not that of a regular close-packed layer. Each Ca(3) octahedron is bisected by a mirror plane, and shares an edges with 2Ca(1) and 2Ca(1′) octahedra, each pair of edges being superimposed in projection. The two Ca(1) octahedra share a point O(6), while the two Ca(1′) octahedra share an edge on the mirror plane. Each Ca(2) octahedron has two vertices pointing in the same direction out of the plane of the diagram. Pairs of Ca(2) octahedra, one lying above the mirror plane and one below, are also superimposed in projection, and share an edge with 2Ca(1) and 2Ca(1′) octahedra. Each ring of 6 silicon tetrahedra bridges between 2Ca(3), 4Ca(2), 4Ca(1) and 4Ca(1′) octahedra.

Each CO_3 triangle is seen end-on, and shares oxygens with 2Ca(1′) and one Ca(3) above and 2Ca(1) and one Ca(3) below the plane of symmetry. When the CO_3 group is assigned one of the two possible orientations, the Ca(1) octahedron of *I*2/*m* splits into two types in *Im*, denoted Ca(1) and Ca(1′). The Ca(1′) octahedra share an apex of the carbonate triangle whereas the Ca(1) octahedra are attached to an edge opposite the apex (Fig. 3).

Figs. 4 and 5 show calcium and silicon layers viewed normal to (101). The calcium–oxygen layer can be idealized [Fig. 4(*a*)] as an infinite sheet of octahedra linked by shared edges. Defects occur where the six-membered rings of silicon tetrahedra are attached above and below these octahedral sheets. A more serious deviation from ideality is caused by the distortion of the Ca(1) and Ca(3) octahedra at the junction with CO_3 groups shown by dotted lines. Pairs of adjacent Ca(1) octahedra are pushed apart by a CO_3 triangle which utilizes one O(7) oxygen from each

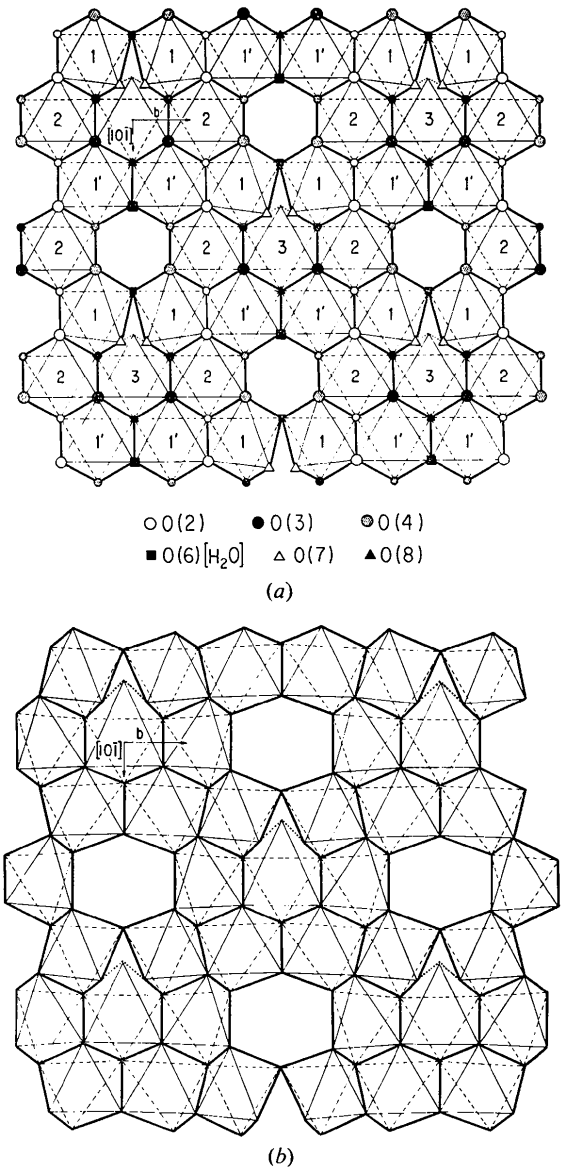

Fig. 4. Idealized (*a*) and actual (*b*) projections normal to (101) showing the linkage of the calcium–oxygen polyhedra (continuous and dashed lines) and the CO_3 groups (dotted).

octahedron. The CO_3 triangle is completed by an O(8) oxygen which forms part of a Ca(3) and two Ca(1′) octahedra.

Fig. 5 shows the silicate layer both (*a*) idealized and (*b*) actual. The Si_6O_{18} rings are severely distorted from an ideal arrangement with sixfold rotation symmetry. Two tetrahedra point up, two point down, and two tetrahedra have one horizontal edge and one vertical edge. The CO_3 triangles lie in the gaps between the Si_6O_{18} rings and appear as isosceles triangles because they are inclined to the plane of projection.

From Tables 2 and 3 it may be seen that the thermal parameters are anomalously high only for atoms forming the CO_3 group and neighboring polyhedra. Accordingly it may be assumed that much of the structure approximates to *I*2/*m* symmetry and that perturbation occurs only for the CO_3 group and its neighbors.

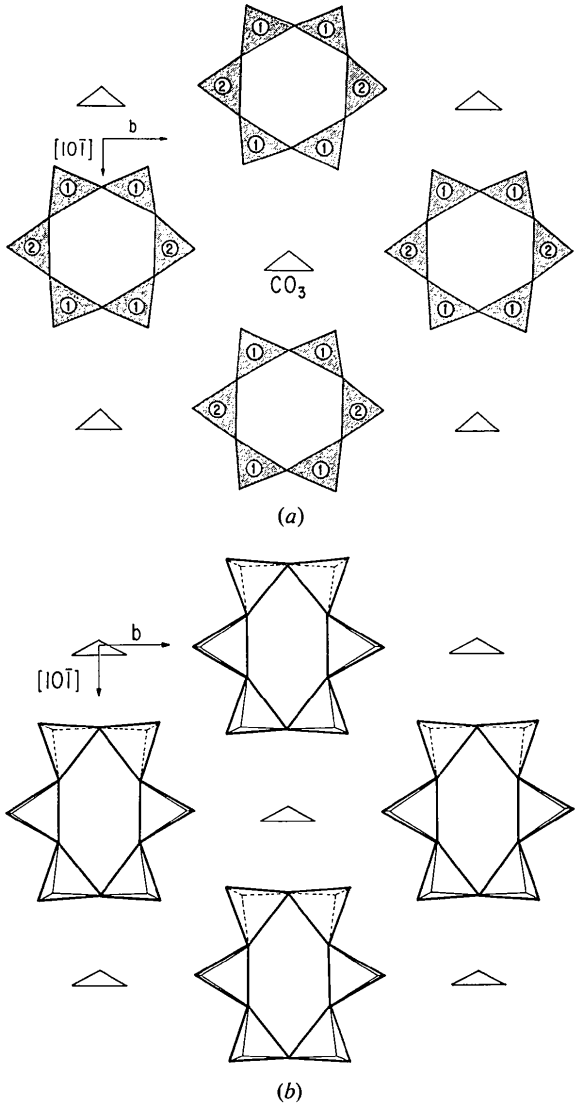

Fig. 5. Idealized (*a*) and actual (*b*) projections normal to (101) showing the position of Si_6O_{18} rings and CO_3 triangles.

A difference Fourier synthesis calculated after the isotropic thermal parameter refinement contained a large residual peak near Ca(3) (4·6 e Å^{-3}). The subsequent anisotropic thermal parameter refinement absorbed this error and suggests displacement of the Ca(3) atom in the plane connecting the oxygen atoms of two CO_3 groups. This displacement would reduce the seemingly long Ca(3)–O(7) distance (2·87 Å). The Ca(3) atom had a maximum root-mean-square displacement of 0·211 (3) Å directed 30 (2)° from the Ca(3)–O(7) bond direction. A similar argument can be made for the short Ca(1)–O(7) distance (2·25 Å), where Ca(1) has a maximum root-mean-square displacement of 0·146 (1) Å directed 24 (2)° from the Ca(1)–O(7) bond direction. The anisotropic thermal parameters of O(7) also behaved peculiarly being nonpositive definite and having an unusually high maximum root-mean-square displacement of 0·41 (1) Å.

Fig. 6 illustrates the composition and distortions of the calcium coordination polyhedra. Ambiguities arise in the definition of these polyhedra because of the CO_3 problem. For Ca(1) there are two possible octahedra, Ca(1) and Ca(1′), which differ only by the atom contributed by the CO_3 [O(7) or O(8)]. For Ca(3) there are three possibilities, all containing four O(3) atoms (related by 2/*m*), but completing the polyhedra in one of three ways: (1) by an O(8) [Ca(3)–O(8) 2·36 Å] and two O(7)'s [Ca(3)–O(7) 2·87 Å], (2) by four O(7)'s [Ca(3)–O(7) 2·87 Å] or by two O(8)'s [Ca(3)–O(8) 2·36 Å]. Two O(5) atoms also approach within 2·90 Å of Ca(3), but lie outside the faces of the less distorted polyhedra formed by the above combinations. For convenience, the Ca(3) polyhedron was described earlier as an octahedron.

For Ca(1) and Ca(2) all of the observed Ca–O distances fall in the range expected for octahedrally coordinated calcium. A seventh atom, O(7), also comes within 2·95 Å of Ca(1). The Ca(3) coordination number can vary from 6 to 10 depending on the assumed coordination polyhedron. Considering each case separately, the Ca–O bond distances all seem to be reasonable. The errors in these distances must be underestimated because of the positional uncertainty in Ca(3) and O(7).

In general, the distortions of the calcium coordination polyhedra are consistent with electrostatic bonding in which cation–cation repulsion causes shortening of shared edges.

Exceptions occur for O(2)–O(7) whose 3·13 Å distance is constrained by the small size of the CO_3 group, and for O(4)–O(6) for which an explanation is not obvious.

The water molecule O(6) forms part of a shared edge linking two Ca(1) octahedra. Oxygen–oxygen close contacts occur as follows: O(6)–O(8) 2·79 Å, O(6)–O(5) 2·82 Å, O(6)–O(1) 3·00 Å and O(6)–O(4) 3·12 Å. If the two sp^3 orbitals containing the lone-pair

electrons are directed toward two Ca(1) atoms the hydrogen atoms would point into a cavity located between two Si_6O_{18} rings. Three oxygen–oxygen close contacts occur [O(6)–O(5) and two O(6)–O(1)] by which the water molecule could bind two Si_6O_{18} rings. Although the O–O distances are in the possible range for hydrogen bonding, the OH···O angles would show large deviations from linearity. Valence-balance rules predict that the water molecule should be hydrogen-bonded to two O(4)'s related by a mirror plane, but the observed O(6)–O(4) distance seems long for a strong hydrogen bond. Hydrogen bonding to O(8) would show serious deviation from the expected tetrahedral sp^3 configuration of a water molecule.

Fig. 7 shows the Si_6O_{18} ring along with important interatomic distances and angles. The observed distortions in the ring can be explained by the *d–p* π-bonding theory proposed by Cruickshank (1961) and a corollary to the above rules proposed by Pant & Cruickshank (1967). Brown & Gibbs (1969) found that Cruickshank's ideas were consistent with data for many silicates. Particularly noteworthy for scawtite is the large difference between bridging and non-bridging Si–O distances [Si–O(br) = 1·64 Å and Si–O(nbr) = 1·59 Å], which correlates with the low electronegativity of the Ca atoms and the small values of the bridging Si–O–Si angles.

The birefringence of scawtite is consistent with the structure model. The lowest refractive index lies at 60° to the *c* axis of the *I* cell in the acute angle, which is close to the normal to the mean position of the CO_3 group.

There is no obvious explanation of the {010} cleavage reported by Murdoch (1955) or the $\{\bar{1}01\}$ cleavage, both transformed to the *I* cell, reported by Tilley & Hey (1930). Actually the structure of scawtite is bonded in such a complex manner that prediction of planes of weakness is very uncertain.

The breakdown of scawtite to wollastonite at high-temperature must involve loss of CO_2 and reconstitution of the Si_6O_{18} rings into $(SiO_3)_\infty$ chains.

In conclusion, all three members of the calcium carbonate silicate group have complex bonding of silicate and carbonate groups by calcium atoms in distorted octahedral coordination. Apart from these local factors, there is no structural resemblance between them.

We thank Romano Rinaldi for the preliminary X-ray study. We also thank the Donors of the Petroleum Research Fund, administered by the American Chemical Society, for a grant-in-aid.

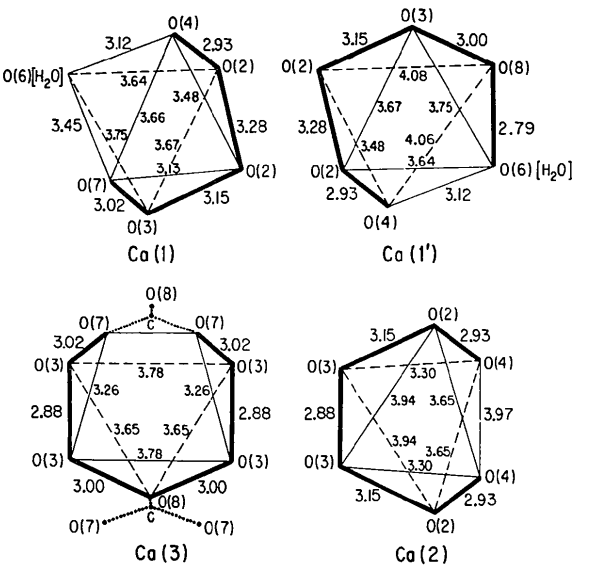

Fig. 6. Shapes of coordination polyhedra around calcium. See text for uncertainties concerning O(7) and O(8). Shared edges are shown by thick lines.

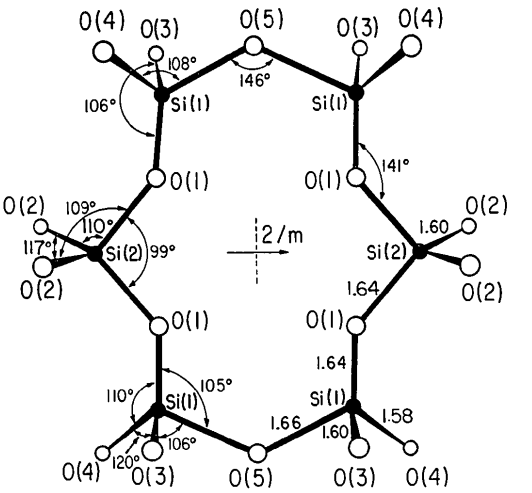

Fig. 7. Geometry of the Si_6O_{18} ring.

References

Brown, G. E. & Gibbs, G. V. (1969). *Amer. Min.* **54**, 1528–1539.

Burnham, C. W. (1962). *Lattice Constant Refinement.* Carnegie Inst. Wash. Yearbook 61, 132–135.

Chao, G. H. (1972). *Amer. Min.* **57**, 765–778.

Cromer, D. T. (1965). *Acta Cryst.* **18**, 17–23.

Cromer, D. T. & Mann, J. B. (1968). *Acta Cryst.* A**24**, 321–324.

Cruickshank, D. W. J. (1961). *J. Chem. Soc.* pp. 5486–5504.

Louisnathan, S. J. & Smith, J. V. (1970). *Z. Krystallogr.* **132**, 288–306.

McConnell, J. D. C. (1955). *Amer. Min* **40**, 510–514.

Murdoch, J. (1955). *Amer. Min.* **40**, 505–509.

Pant, A. K. & Cruickshank, D. W. J. (1967). *Z. Krystallogr.* **125**, 286–297.

Smith, J. V. (1953). *Acta Cryst.* **6**, 9–18.

Smith, J. V., Karle, I. L., Hauptman, H. & Karle, J. (1960). *Acta Cryst.* **13**, 454–458.

Tilley, C. E. & Hey, M. H. (1930). *Miner. Mag.* **22**, 222–224.